Journal of Magnetism and Magnetic Materials 410 (2016) 187–197

Contents lists available at ScienceDirect

Journal of Magnetism and Magnetic Materials

journal homepage: www.elsevier.com/locate/jmmm

Computing the blood brain barrier (BBB) diffusion coefficient: A molecular dynamics approach

Amir Shamloo *, Maysam Z. Pedram, Hossein Heidari, Aria Alasty *

Department of Mechanical Engineering, Sharif University of Technology, Azadi Street, Tehran, Iran

ARTICLE INFO

Article history:
Received 23 December 2015
Received in revised form
17 February 2016
Accepted 4 March 2016
Available online 5 March 2016

Keywords:
Magnetic nanoparticle
Forced steering
System dynamics identification
Discrete medium
Continuous medium

ABSTRACT

Various physical and biological aspects of the Blood Brain Barrier (BBB) structure still remain unfolded. Therefore, among the several mechanisms of drug delivery, only a few have succeeded in breaching this barrier, one of which is the use of Magnetic Nanoparticles (MNPs). However, a quantitative characterization of the BBB permeability is desirable to find an optimal magnetic force-field. In the present study, a molecular model of the BBB is introduced that precisely represents the interactions between MNPs and the membranes of Endothelial Cells (ECs) that form the BBB. Steered Molecular Dynamics (SMD) simulations of the BBB crossing phenomenon have been carried out. Mathematical modeling of the BBB as an input-output system has been considered from a system dynamics modeling viewpoint, enabling us to analyze the BBB behavior based on a robust model. From this model, the force profile required to overcome the barrier has been extracted for a single NP from the SMD simulations at a range of velocities. Using this data a transfer function model has been obtained and the diffusion coefficient is evaluated. This study is a novel approach to bridge the gap between nanoscale models and microscale models of the BBB. The characteristic diffusion coefficient has the nano-scale molecular effects inherent, furthermore reducing the computational costs of a nano-scale simulation model and enabling much more complex studies to be conducted.

1. Introduction

Even in the 21st century, many studies are focused on investigating biological systems inside the human body and also animal bodies. In this area, the Blood Brain Barrier (BBB) has attracted a considerable amount of attention. The importance of the BBB could be clearly represented in research studies carried out on brain diseases. In fact, treatment for some of these diseases requires a precise analysis of the BBB. Therefore, nowadays a lot of research has been conducted on the modeling of the BBB [8].

The idea of a BBB that separates the blood and brain was developed about 100 years ago. The BBB is created at the same level of the cerebral capillary endothelial cells by the formation of tight junctions. It has the largest surface area for exchange which measures around 12–18 m^2 in an adult human. No brain cell is farther than about 25 mm from a capillary, so once the BBB is crossed, diffusion distances to neurons and glial cell bodies for solutes and drugs are short. Thus, delivery of drugs to all brain cells is done by designing drugs that are optimal for crossing through the BBB [1].

The structure of the BBB has not yet been understood completely and an ideal model of the BBB is desirable. Some research has been carried out on the modeling of the BBB. In Ref. [12], a BBB model with the use of a microfluidic chip has been investigated. The barrier function has been modulated both mechanically by exposing the cells to fluid shear stress, and biochemically, by stimulating the cells with tumor necrosis factor alpha (TNF-), respectively. Electrodes have also been integrated in this chip for analyzing barrier tightness through the measurement of transendothelial electrical resistance (TEER) [12]. Alongside this microfluidic modeling, a few other models have also been proposed for in vitro BBB modeling that have been studied in Refs. [23,25,20,11]. In Ref. [24], using silver nano-particles, micro-particle crossing through the BBB has been studied in detail. In this study, it has been experimentally shown that the percentage of crossing success for the smaller nano-particles through the BBB is higher than the micro particles. Although the size of nano-particles crossing is significantly larger than micro particles (2.76% versus 0.10%), this value could be possibly improved by the application of external forces on the nano-particles. Creating an in vitro BBB with the use of culturing methods would be a good idea to test the permeability of nano-particles. Since measuring the dynamics of particles during such a study is complex and hard to do, analyses based on

* Corresponding authors.
E-mail addresses: shamloo@sharif.edu (A. Shamloo), aalasti@sharif.edu (A. Alasty).

http://dx.doi.org/10.1016/j.jmmm.2016.03.030
0304-8853/

static data would be the only possibility. For this reason studies based on image has been the subject of a research that was conducted in Ref. [5]. The trapping of nano-particles inside the layer is another issue that has been addressed in Ref. [24]. In fact, it shows that many of the particles may be situated in the membrane and it requires too much time for them to diffuse to the other site, moreover, nano-particle, due to their small size may be up taken by the cells instead of being able to cross through the extra cellular medium. The up-taking of nano-particles into the cells has been considered in Ref. [13]. In this case an external force may help free these involved nano-particles.

The major problem in drug delivery to the brain is the limitations of drug penetration due to the presence of the BBB. In fact, the BBB acts as a dam to prevent the entrance of toxic agents, due to the brain's endothelial cells that are located on the vessel walls. It shows some important features such as the presence of tight junctions between the cells and the absence of fenestrations that together restrict the crossing of compounds from the blood into the brain. The traversing ability of the membrane affects the diffusion of drugs from the blood into the brain. Efforts to overcome this traversing effect in vivo, have been focused on changing the characteristics of this barrier that alter the characteristics of the drug. Beside endothelial cells, tight junctions at the BBB have been artificially opened using osmotic pressure and RMP-7 as an administrator of bradykinin analogs. This results in the entrance of toxic and unwanted molecules into the CNS and may result in serious damage [19].

Delivering drugs to the brain with the use of magnetic nanoparticles (MNPs) may provide a significant advantage over current strategies. Magnetically controlled chemotherapy under MRI is a novel technique which is based on magnetic forcing of a therapeutic magnetic microcarrier through an MRI system. Moreover, the surface of these nanoparticles can be bio-conjugated with specific antibodies so that the immune system would not be able to detect them. Crossing through the BBB may be due to the recognition of these nanoparticles by the receptor at the surface of the endothelial cells of the BBB. Since using MRI systems is a very expensive approach, most of the studies are concentrated on numerical and computational modeling methods in order to reduce the risk and uncertainty inherent in the nanoparticle development process. This project deals with the simulation of super paramagnetic nanoparticles crossing the BBB via a hybrid approach: mechanical steering driven by a magnetic force field combined with chemical surface functionalization [14]. For special single nano-particles coated with gold, crossing through the BBB by means of special force profiles has been done. This research has been focused on the MD computation of the extracted force profiles in order for the particle to traverse in constant velocities across the membrane. This study has been furthered in this paper using a wide range of crossing velocities [27].

In this study the diffusion resistance and permeability of the membrane is computed based on the molecular-scale data. In this way, the BBB has a precise dynamic model originated from basic and molecular size simulations. One of the most important issues in MD modeling is the stochastic and random behavior of the molecular simulation that is mainly produced by Brownian force. In this study, MD simulations have been carried out several times with variable parameters. The uncertain behavior of the system has been precisely included in the linear model. Since the MD external forces are based on steered MD forces, therefore computation of the diffusion coefficient needs to be based on a method compatible with this parameter. There are many traditional biasing methodologies [10] for this propose such as umbrella sampling [2,4]. In this article, we use a novel technique that is based on reverse and forward Steered Molecular Dynamics (SMD) simulation such as the ones used in Refs. [15,16,18] and Ref. [22] for populating high energy regions of potential energy and crooking the fluctuation relations in order to estimate the free energy barrier for the particles crossing through the BBB. All these procedures have been gathered in [9] completely for the purpose of computing a diffusion coefficient using MD simulations.

In the next section, different nanoparticle diffusion scenarios are considered and the corresponding mathematical background for the calculation of a general diffusion coefficient in each case is given. The main emphasis of this research is on employing the SMD based method for the extraction of a diffusion coefficient. The third section explains the strategies used for the calculation of the diffusion coefficient. The fourth and fifth sections describe the molecular dynamics simulation and mathematic modeling of the BBB membrane. Section 6 is dedicated to results.

2. Biological strategies for crossing through the BBB

There are several potential routes for permeation across the BBB as described below and explained in detail in Ref. [1]:

- Passive partitioning into the brain

  A wide range of lipid-soluble molecules can diffuse through the BBB and enter the brain passively. There is a general correlation between the rate at which a solute enters the CNS and its solubility, usually determined as the logD octanol/buffer partition coefficient at a pH of 7.4 (Fig. 1a).

- Solute carriers (SLCs) in the BBB

  The barrier to paracellular diffusion potentially isolates the brain from many essential polar nutrients such as glucose and amino acids necessary for metabolism and therefore the BBB endothelium must contain a number of specific solute carriers (transporters) to supply the CNS with these substances (Fig. 1c).

- ATP-binding cassette transporters (ABC transporters) in the BBB

  When comparing brain penetrance with lipid solubility (lipophilicity), a large number of solutes and drugs have a much lower CNS entry rate than might be expected from their logD. These substances and many of their metabolites are actively effluxed from the brain and the capillary endothelium forming the BBB by the members of the ABC transporter (ATP-binding cassette) family (Fig. 1b).

- BBB transport of macromolecules

  Transcytosis of macromolecules across the BBB via endocytotic mechanisms provides the main route by which large molecular weight solutes such as proteins and peptides can enter the CNS intact (Fig. 1d).

- Cell movement across the BBB

  Cells from the bone-marrow derived monocyte lineage enter the brain during embryonic development and become resident immunologically-competent microglia. Mononuclear leukocytes, monocytes and macrophages are able to be recruited to the CNS in pathological conditions, and play roles complementary to those of the resident microglia; in some cases they may transform into a microglial phenotype (Fig. 1e).

  Moreover, physical methods of crossing are expressed as:

- Ultrasound-induced Blood Brain Barrier opening

  In this method, temporary opening of the BBB is carried out by means of focused ultrasound sonication (FUS) in the presence of microbubbles. Therefore, it allows systemically administered agents to enter the brain. Both the targeted brain region and the size distribution in the injected microbubble volume affect the efficiency of FUS induced BBB opening [7] (Fig. 1f).

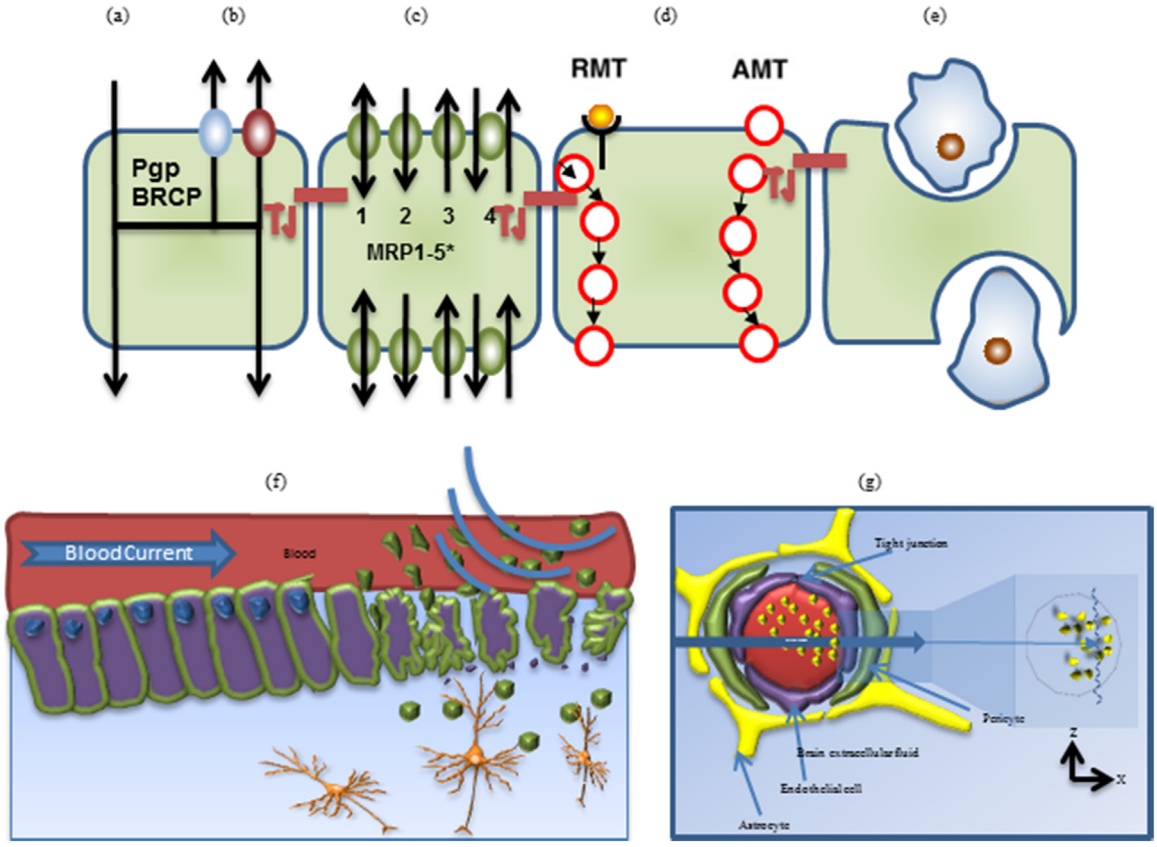

Fig. 1. Routes of biological (a–e) and physical (f and g) transport across the BBB [1].

- Using external forces and applying to nanoparticle

Applying force to nano-particles is one of the solutions for crossing nano-particles through the BBB. By selecting a magnetic particle and applying a suitable magnetic field intensity, a magnetic force is applied to NPs which affects the trajectories of nano-particles. The major issue associated with this method is to find the best magnetic force profile which must be applied to the nano-particles (Fig. 1g).

3. Preliminary mathematics

Diffusion is defined as the phenomenon of material transport by atomic or particle flux from regions of high concentration to those of lower concentrations. Diffusion coefficients are assigned in several cases within the different physical states of matter, what is usually considered as diffusion is either self-diffusion which happens quite randomly and is independent to any specific sort of gradient or outer force field, in this case the diffusion coefficient is dependent to the lattice structure geometry, the inter atomic distances and also the jump frequencies. The other kind of diffusion which is the main intention of the present study, is the one which happens under certain forced conditions, which is called inter diffusion, however the physical understanding of the diffusion phenomenon of a particle passing through a barrier which yields to the calculation of the diffusion coefficient is quite the same for both cases.

3.1. Fick's laws and the Nernst–Einstein equation for diffusion under concentration gradients

In this type of diffusion, which happens in the form of mass or molar fluxes of atoms driven by concentration gradients, the phenomenon happens in the form of different mechanisms governed by derivations and modifications of the main form of fick's first law and fick's second law for unsteady conditions [10]:

$$W_{Ax} = -D_A\left(\frac{dC_A}{dx}\right) \tag{1}$$

In this equation $\boldsymbol{C_A}$ is the concentration of substance $\boldsymbol{A}$ and $\boldsymbol{D_A}$ is the diffusion coefficient and diffusion is considered to be happening in only one direction, that is, along the x axis. The Nernst–Einstein equation which is derived from the Darken's equation, gives us a relationship between this diffusion coefficient and the free energy of the system and thus its temperature:

$$n'_{Ax} = \frac{-n_A B_A}{N_0}\left(\frac{dG_A}{dx}\right) \tag{2}$$

In this equation $\acute{n}_{\boldsymbol{Ax}}$ is the flux of $\boldsymbol{A}$ atoms diffusing in the x-direction and $\boldsymbol{G_A}$ is the partial molar free energy of $\boldsymbol{A}$ and $\boldsymbol{N_0}$ is the Avogadro's number and $\boldsymbol{B_A}$ is the mobility of $\boldsymbol{A}$ atoms in the energy gradient field. X_A is the mole fraction of $\boldsymbol{A}$ and $\mathbf{a_A}$ is the concentration of $\boldsymbol{A}$. The diffusion coefficient is calculated with the use of the following equation:

$$D_A = B_A k_B T\left(\frac{d\log a_A}{d\log X_A}\right) \tag{3}$$

This relation can also be written in the form of the Arrhenius equation. Also similar integrated equations have been extracted for the other two phases of matter that are the liquid and gas phases. For the porous media situation the Eq. (4) has been given:

$$D_{eff} = \frac{D\omega}{\tau} \tag{4}$$

where $\boldsymbol{\tau}$ is turtuosity, the value of which depends on the consolidation state of the particle which is tending to diffuse into the

porous media and ω is the lattice void fraction. For a particle with a spherical geometry such as the spherical gold nanoparticle studied in this research, the later forms of the diffusion coefficient mentioned above can be written as follows:

$$D_T = \frac{1}{2d}\liminf\frac{\langle x^2\rangle}{t} \tag{5}$$

The simplification of the above equation with the use of Langevin equations yields to the equation bellow:

$$D = \frac{k_B T}{\eta R_D a} \tag{6}$$

where η is the membrane shear viscosity, one of the transport coefficients and R_D is an approximation of the sphere or near sphere radius and α is a constant depending on boundary conditions. Estimations of the value of this coefficient somehow determine the moving pace of the bio particles. For the diffusion of a protein in a membrane this value is about 10^{-9} cm^2/s whereas for lipids tending to diffuse through a gel-like membrane, this value is about 10^{-8} cm^2/s. Diffusion usually happens either in the form of self-diffusion which is regardless of any external force field and does not require any simulation data such as SMD data or etc. to be derived from and is in fact only dependent on the structural and physical properties of the desired system, or it might happen in the form of inter-diffusion, the general governing equations for which have been mentioned in this section and will be demonstrated specifically for the SMD case in the following two sections.

3.2. Methods for calculating the diffusion coefficient with the use of SMD data

The other form of diffusion that also carries some analogies with the first form, is the one which happens under certain forced and steered, non equilibrium conditions. calculation of a diffusion coefficient in the later form of diffusion which is the main focus of the present study requires a considerable amount of MD simulation data and will be dealt with using the mathematics of this part described in this section and the next one. The required variables for the evaluation of the diffusion coefficient which are the force and position through time data collected from the SMD simulations, the spring constants of the SMD atoms, also the pulling velocity and the system temperature have to be collected from the simulations. In order to calculate the diffusion coefficient, at the first step a few fast non-equilibrium SMD pullings have been performed on the particle in both the forward and reverse directions through the membrane and thus this method is referred to as the FR method, then, the variables described in the above section were collected and using Eq. (7) followed by the subtraction of the instantaneous biasing potentials calculated in Eq. (8), we have calculated the work difference for both the forward and reverse paths with the use of Eq. (9). The dissipated work difference is then calculated with the use of Eq. (10) [9].

$$W(t) = -k\int_0^t vdt'\big(z(R(t')) - z_0 - vt'\big) \tag{7}$$

$$V(R, t) = \frac{k}{2}\big(z(R) - z_0 - vt\big)^2 \tag{8}$$

$$\Delta W(t) = W(t) - V\big(R_t, t\big) \tag{9}$$

$$\Delta W_d(z) = \frac{1}{2}\big(\langle\Delta W_z\rangle_P + \langle\Delta W_z\rangle_R\big) \tag{10}$$

Here in, the above procedure has been carried out for a relatively wide range of pulling velocities and finally, having the system temperature and a set of points in the dissipated work difference versus velocity plane, the diffusion coefficient is calculated with the use of a linearized model for diffusion calculation and the simulation data. the slope of the given line is proportional with the diffusion coefficient, and thus the coefficient can be calculated using Eq. (11):

$$\Delta W_d = \left(\frac{\Delta z}{(D(z)\times\beta)}\right)v \tag{11}$$

where $\Delta(z)$ is the distance swept by the particle under the action of the constant velocity force and:

$$\beta = \frac{1}{k_B T} \tag{12}$$

where k_B is the Boltzmann constant. Now we are able to calculate an approximation of the diffusion coefficient of the BBB, which can be then used in further calculations regarding the force field required for the delivery of drugs into the brain. The procedure described above, closely depends on whether the SMD pulling paths are near-equilibrium, in the following section a brief description of a modified and more precise method established by Ref. [4] has been given and our desired diffusion coefficient has also been calculated with the use of this procedure. At the first step a few fast non-equilibrium SMD pulling are performed on the particle and the FR method is again applied. Next, an average amount of work for both directions is extracted from either the Gaussian work distribution functions of the collected data or from the density of the plots showing work versus distance. We take advantage of the knowledge we have regarding the characteristics such as maximum, average and variance of a Gaussian distribution in order to decrease the number of F–R pulling simulations, that is, having a few pulling paths we can predict the overall shape of the distribution function with a good precision. Now that we have the values for W_F and W_R at every arbitrary z we can find the average dissipated work and thus we can find the diffusion coefficient D:

$$W_d = \frac{(W_F + W_R)}{2} \tag{13}$$

$$D = \frac{k_B T v}{\left(\frac{dW_d}{dz}\right)} \tag{14}$$

As it can be seen in the above equation, the position dependent diffusion coefficient is not only a function of the temperature and pulling velocity but it also is a function of the positional rate of change of the dissipated work during consecutive pullings. Herein v is the pulling velocity and D can be calculated for every desired z with the use of the above equations.

4. Crossing of a nanoparticle through the BBB

In our MD simulations, nano-particles were modeled as rigid bodies. In fact magnetic particles such as Fe_3O_4 would be suitable for this purpose. In this way, the Thiol molecule that is widely used to connect gold atoms to organic molecules was also used in this study to create the bonding in between nano-particles and insulin molecules. The atomic bond between nano-particle atoms and thiol molecules was made using the SPARTAN software. The simulation was carried out in [27] to investigate the crossing of nano-particles through the BBB and was done for a 2 nm in diameter nano-particle crossing a 100 Å × 100 Å POPC membrane in 310 K (the biological temperature of the human body) using the SMD method. The simulation was carried out. After 50 ps of relaxation, the nano-particle crossed the membrane with a constant

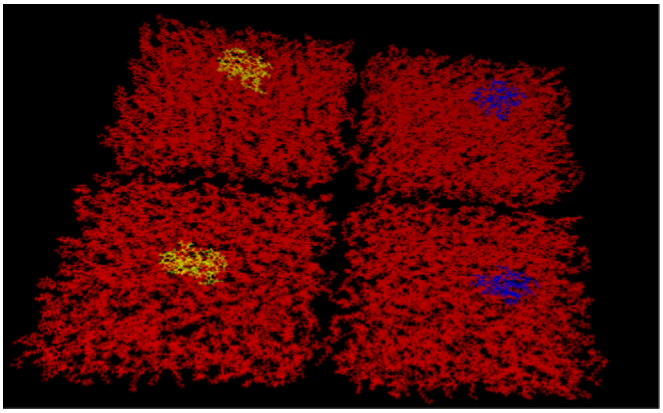

Fig. 2. 200 Å × 200 Å phospholipid membrane with 4 insulin receptors placed on it.

velocity of **5 Å/Step** and the force exerted on the nano-particle was recorded. The new simulation repeated the same procedure and constant velocity pulling force was applied to the nano-particles described in the above sections in order to move them through the membrane and then again, the force and position data were extracted. The distance in between the nano-particle and the membrane has been kept constant and the pulling velocity in the simulations varies in a relatively wide range, from **0.0001 Å/Step** to **0.06 Å/Step** and the same temperature and periodic conditions.

4.1. Molecular modeling and simulation

4.1.1. BBB Structure (main membrane)

The brain microvasculature is composed of three cellular elements which are the BBB endothelial cells, astrocyte end-feet, and pericytes. Tight junctions (TJs) that are present in the gap between the cerebral endothelial cells, create a diffusive barrier, which selectively avoids the entrance of most blood-borne substances to the brain. The BBB endothelial cells differ from endothelial cells in the rest of the body by the absence of fenestrations, more extensive tight junctions (TJs), and sparse pinocytic vesicular transport. In this study, only the cell membrane is modeled, because there is no significant resistance against the nano-particle when it crosses the cytoplasm. Of course, this assumption is for the case that the nano-particle is crossing the cell membrane and not the junctions between the cells. In case of crossing through the tight junctions, a more complicated interaction should be modeled [3].

4.1.2. Endothelial cell membrane: a phospholipid bilayer

One major class of lipids are phospholipids which are vital components of all cell membranes as they can form lipid bilayers. Most of the phospholipids contain diglyceride, a phosphate group, and a simple organic molecule as choline. Lipid bilayers are thin polar membranes that are made of two layer lipid molecules. These membranes are flat shells that shape a continuous barrier around the cells. Phospholipids are usually named with 4 letters. The first two letters are the abbreviations of the two fatty acids in the tail. The last two letters are the abbreviations of the names of the hydrophilic heads. Phospholipids are categorized by their two last letters. In the literature, DMPC (DiMyristoyl PhosphoCholine) and POPC (Palmitoyl Oleyl Phosphatidyl Choline) are mostly used to simulate the BBB. Therefore, a combination of these phospholipids was chosen in the present project.

4.1.3. Putting insulin receptors on the membrane

The transport of the nano-particle through the BBB is mediated by specialized ligands coated on the nano-particle surface, and receptors covering the membrane including the Insulin receptor (IR) or the Transferrin receptor (TfR), which are highly expressed on the capillary endothelium of the brain. In the present study, insulin was used as the ligand coating the nano-particles and insulin receptors were used to cover the membrane surface. The insulin receptor (IR) is a type of transmembrane receptor that is activated by insulin such as IGF I, IGF II and are included in the large class of tyrosine kinase receptors. Metabolically, the insulin receptor plays an important role in glucose homeostasis regulation. Interactions of the complete domains of insulin and insulin receptors is complicated chemically and physically. Therefore, we have modeled the ectodomain of the receptor molecules as the main domain affecting this interaction. Ectodomain is the domain of the receptor protein that extends into the extracellular space. Insulin receptor ectodomain with pdb ID 3W11 was selected from the Protein Data Bank (www.rcsb.org). Chains A and B were cut from the molecule. These two chains are active parts of the ectodomain. Therefore, the ligand on the nano-particle will bind to these chains. Arranging the receptors on the membranes was done in VMD (Visual Molecular Dynamics software). First, both membrane and receptor were loaded in VMD and the receptor was moved so that it locates in the middle of the surface of the membrane. Each receptor is put in a 100 Å × 100 Å membrane and two 15 Å layers of water sandwich them as shown in Figs. 2 and 3. Thus, for a 200 Å × 200 Å phospholipid bilayer, the 100 Å × 100 Å membranes and receptors were merged and assembled in VMD. Fig. 3 shows a 200 Å × 200 Å membrane with 4 receptors on it with the 15 Å layers of water.

4.1.4. Nanoparticle modeling

In this study, nano-particles were modeled as rigid bodies in the MD simulations. In this way, the only interactions included in the simulations are the nonbonded interactions between nano-particle atoms and the biological molecules such as the electrostatic, hydrogen bonding and van der Waals interaction forces; in other words, there are no interactions between the nano-particle atoms. This assumption was made since the atomic bonds between the nano-particle metallic atoms are much stronger than the chemical bonds between the nano-particle atoms and the other organic atoms present in this study. The Thiol molecule that is widely used to connect gold atoms to organic molecules was also used in this study to create the bonding in between gold nano-particles and insulin molecules. The atomic bond between gold atoms and thiol molecules was made using the SPARTAN software. Thus we have considered the quantum mechanical interactions of the gold atoms and the sulfure atoms on the thiol molecules. Fig. 4 shows a 2 nm gold NP coated with 18 thiol residues after 100 ps relaxation time. Figs. 5 and 6 also show a 10 nm gold nano-particle coated with 18 insulin segments and the POPC membrane with the 2 nm and 10 nm gold NP above it, respectively.

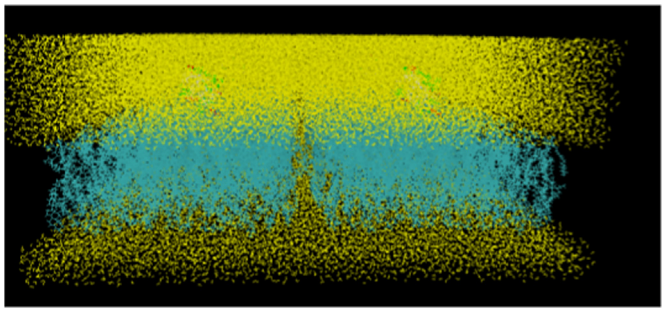

Fig. 3. 200 Å × 200 Å phospholipid membrane with 4 insulin receptors placed on it sandwiched with the 15 Å layers of water.

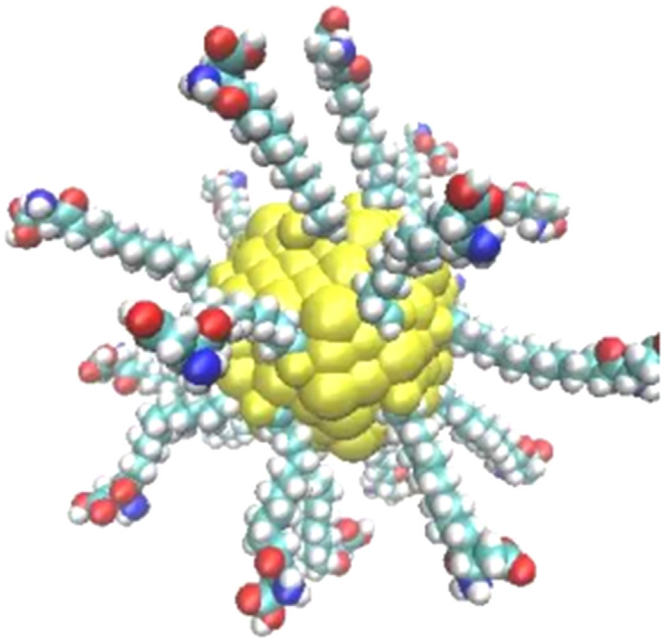

Fig. 4. A 2 nm gold nano-particle coated symmetrically with 18 Thiol residues and relaxed for 100 ps.

4.2. Force profiles

Using MD simulations, we have predicted that coating spherical nano-particles with insulin would be an effective method in facilitating the procedure of their crossing through the membrane. This result was obtained using the SMD method, and crossing the nanoparticle through the BBB with different velocities. The velocity of the nano-particle varies between 0.00005 Å/fs and 0.030 Å/fs. Fig. 7 shows the interaction forces recorded during the simulation.

5. Mathematical modeling of the BBB

5.1. Identification of the BBB system

System identification is an algorithm to express systems in mathematical equations format in order to describe the dynamic behavior of a system in either the time or frequency domain. It's also not restricted to special systems and it includes industrial processes, economic and even biological systems. There are globally two approaches in system identification; gray box and black box. The approach of gray box for modeling is based on physical knowledge with data gathered from the system; physical knowledge gives a structure of the mathematical equation with a few unknown parameters. These parameters have to be estimated by identification methods [21]. The black box approach is based on no model and most of the algorithms are categorized in this type. In this study, we don't have any information about the dynamics of the BBB and it lies in the category of black box system identification. There are two algorithms in systems identification; 1) input–output identification and 2) output-only identification. In the later, system parameters must be estimated based on just the output [6], however in the first method, parameter estimation accomplishes with both the input and output. Obviously, including more information of the system causes less variance of estimations. To convey the identification, we have to first excite the system with suitable input time series data. In this case based on MD simulations, the velocity of the nano-particle is fixed and the particle-membrane interaction force has been extracted. The velocity of the nano-particle varies between 0.00005 Å /fs and 0.030 Å /fs. These simulations approximately take around 3 days each, with a 4 core XEON 5650 2.67 GHz server computer. Results of all gathered data from the abovementioned range of velocities are illustrated in Fig. 7. The ***X*** axis of this figure represents the steps of simulation. Each time step is related to a defined sample time which is constant during the simulation.

As it is shown in Fig. 7, for the crossing of nano-particles through the membrane, a special variation and oscillation through time in the actuating force on the surface of the membrane is required. Fig. 8 from a system identification viewpoint is the impulse response of the BBB membrane with velocity as an input and interaction force as an output.

Since each input is related to its output, in this system the output corresponding to an impulse input has been considered. Beside the time response of the system, the frequency domain gives us many other data analysis tools. It can represent the variation of the system dynamics through different frequencies much better. In order to represent the response in the frequency domain, we need to assume a defined transfer function between the inputs and outputs. In this case a transfer function with a maximum of 5 poles and 3 zeros has been considered based on minimizing the model error by means of input-output data parameters estimation. Eq. (15) shows the input-output transfer function. Notice that the input is velocity and the output is the double integrated force.

$$F(s) = \frac{b_3 s^3 + b_2 s^2 + b_1 s + b_0}{s^5 + a_4 s^4 + a_3 s^3 + a_2 s^2 + a_1 s + a_0} V(s) \tag{15}$$

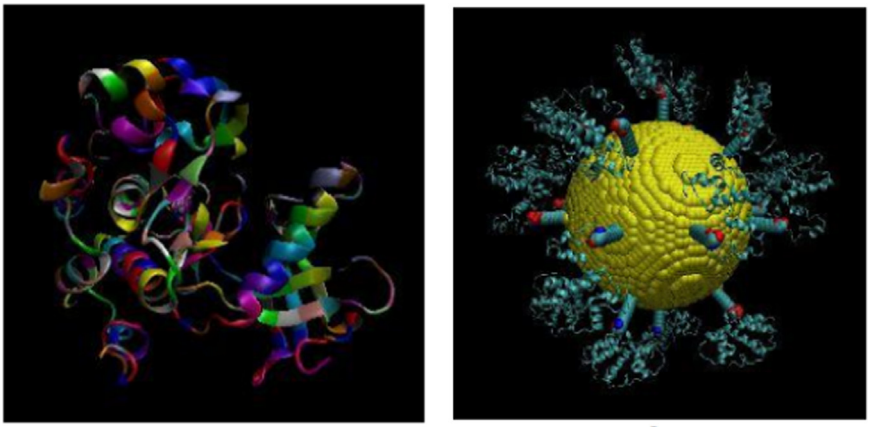

Fig. 5. Schematic representation of (a) human Insulin molecule, and (b) 10 nm gold nano-particle coated with 18 segments each containing 121 residues.

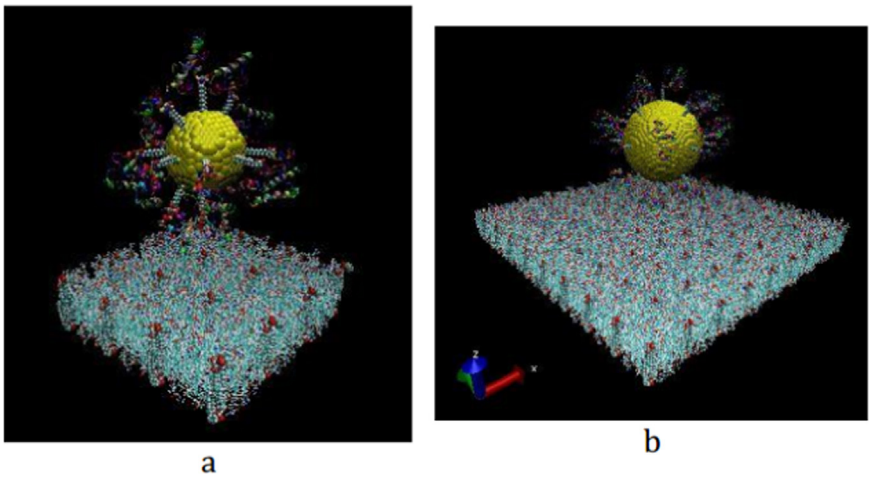

Fig. 6. Schematic representation of (a) 2 nm coated gold nano-particle crossing a 15 nm by 15 nm POPC membrane, and (b) 10 nm coated gold nano-particle crossing a 40 nm by 40 nm POPC membrane.

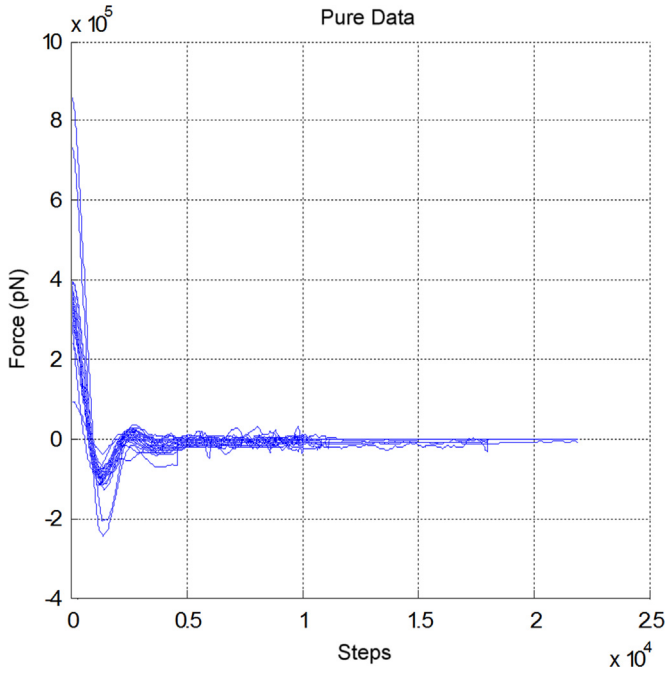

Fig. 7. Interaction force profiles that are exerted by the phospholipid membrane on the gold nano-particle.

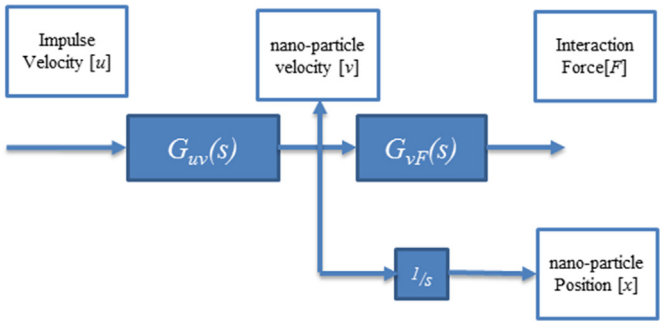

Fig. 8. The system's dynamics diagram showing a schematic of the way transfer functions relate the velocity impulse or any arbitrary velocity input applied to the dummy atoms to the position and force outputs corresponding to the gold nano-particle.

Using the MATLAB identification toolbox and setting arranged input-output data as an iddata, unknown parameters of Eq. (15) are extracted for each dataset. The bode diagram of all system sets are shown in Fig. 9. As it can be seen in this figure, the bode diagram of the dataset includes a region in the frequency domain. In fact, the uncertainty causes this diversity. The important key to modeling is the selection of a linear model with an uncertainty profile.

5.2. Unstructured uncertainty model of the BBB

In the previous section, the system was modeled with a defined dataset. The model has been designed so as to best fit this data. Therefore, according to the system response, a transfer function with a maximum of 5 poles and 3 zeros has been considered. In order to model the uncertainties, we have selected an uncertain model in the form of Eq. (16) [17,26].

$$P(s) = P_{nominal}(s)(1 + \Delta(s)W_t(s)) \tag{16}$$

In which P_{nominal} is the nominal linear system of the uncertainty model, W_t is the term causing uncertainty around the nominal system with a random minimal phase of Δ, having Δ, $\|\Delta\|_\infty < 1$. Fig. 9 shows the bode diagram of the dataset, the nominal system and the uncertainty model. Selection of W_t is one of the main issues. In Eq. (17) a simple way is proposed to select the best frequency domain function. In this method W_t is defined as the upperbound of $\|P/P_{\text{nominal}} - 1\|_\infty < W_t$. In this way, the best nominal plant and frequency domain function of W_t is derived. Fig. 8 shows the diagram of the entire system's dynamics. In this figure, an impulse input is applied to $G_{uv}(s)$ the result is the nanoparticle velocities. The $G_{vF}(s)$ system maps the nanoparticle velocities to the membrane interaction forces. As shown in Fig. 8 it is clear that through the identification procedure of nano-particle velocities, interaction force and position could be available.

Table 1 expresses the parameters computed in the identification procedures. In this table, parameters related to nominal and uncertain transfer functions of both $\boldsymbol{G_{uv}}$ and $\boldsymbol{G_{vF}}$ are presented. Since the sample time of identification is 2 fs, in Table 1 the transfer functions are expressed in descrete domain.

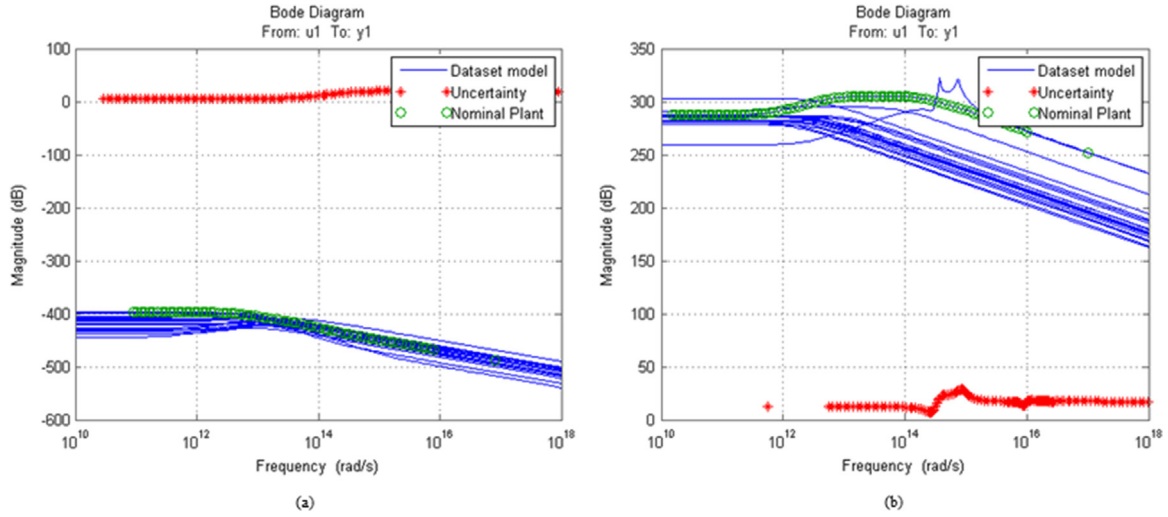

Fig. 9. Bode diagram of (a) the nominal system and uncertainty model of $\mathbf{G_{vF}(s)}$, and (b) the nominal system and uncertainty model of $\mathbf{G_{uv}(s)}$.

6. Results and calculation of the diffusion coefficient

In this part and after the examination of diffusion of the nano-particle in the membrane and identification of a linear model with uncertainty, we are interested in the extraction of a desired parameter which can represent the diffusion characteristic of the membrane, so that we can use this parameter for further calculations regarding the modeling of the BBB. A suitable parameter in this regard is the diffusion coefficient, as mentioned, Our identified linear model has been run for different velocities for 1000 times and in each case the diffusion coefficient has been extracted. The velocity of the nano-particle ranges from 0.0005 Å/*Step* to 0.06 Å/*Step*. The results show that for all velocities, the same diffusion coefficient has been extracted (Eq. (7)–(14)). By averaging the results of all 1000 extractions in a same velocity, the diffusion coefficient is computed. This value is close to 45.6 $Å^2/ns$. In Fig. 10, four samples of the velocity diagrams and interaction force profiles, figured out through at least 40 runs each, have been presented. Fig. 11 shows the variation of the diffusion coefficient as a function of the pulling velocity.

The most important feature of the magnetic behavior of the magnetic nanoparticles is considered to be the magnetic saturation curve. In fact, all the design is restricted to the saturation of nanoparticles and designing in the saturation zone is not valid because it could not be possible to exert computed forces on a nano-particle and it shows a nonlinear magnetic behavior and the maximum force is restricted. In Fig. 12, the magnetization curve for Fe_3O_4/Au core/shell (the commercially used gold nanoparticle) is shown. In this curve the maximum magnetic field is 2. 5[T] and the design parameters must be considered accordingly [28]. The MD simulations described in this paper, used a static magnetic field strength of 1. 5[T] with a maximum spatial gradient magnetic field of 3. 3[$\frac{T}{m}$]. Since the maximum magnetic field value permitted for a nano-particle should not cause saturation (Fig. 12), the effective magnetic field intensities simulated in this work do not exceed 2. 5[T] for core/shell (Fe_3O_4/Au) magnetic nanoparticles.

$$b_z \frac{\partial b_z}{\partial z} = \left[L_b, U_b\right]$$

$$b_z \times 3.\ 3\left[\frac{T}{m}\right] = [2,\ 9]$$

$$0.\ 6 < b_z < 2.5 \tag{17}$$

Based on Eq. (17) above, the magnetic field ($\boldsymbol{b_z}$) must be in a range between 0. 6[T] and 2. 5[T] for the magnetic nanoparticles to cross the BBB membrane. The time of crossing through the membrane in this case has been calculated to be in the range of 1. 5[min]– 7[min]. The required time can be calculated through rescaling the traveling nanoparticles from upper velocity to lower velocities in the same distance and restricted magnetic field. According to these calculations, it is possible to exert low magnetic field with higher duty cycle time and vice versa, while still MNPs can cross the BBB. Hence, the effect of magnetic force field and its gradient can be interpreted in this way that for every desirable crossing time we have a corresponding region of interest in the magnetic force field – magnetic force field gradient plane that could be obtained through the application of these criteria along with the crossing duration consideration. We have carried out this procedure for 1.5, 2.5 and 4.5 min of crossing time and the resulting diagrams are shown in Fig. 13. As could be perceived from this figure, the magnetic field and its gradient are localized in the lower value region for increased time of crossing. Moreover, as we

Table 1
Identified parameters.

	$P_{nominal}$ (s)	W_t (s)
$G_{uv}(s)$	$\frac{6.378e^{14}z - 6.388e^{14}}{z^2 - 1.653z + 0.6572}$	$\frac{6.95z^9 - 6.13z^8 - 2.031z^7 + 4.822z^6 - 1.042z^5}{z^9 - 1.301z^8 + 1.363z^7 - 0.8635z^6 + 0.5709z^5}$ $\frac{+0.2729z^4 - 0.07625z^3 + 0.007149z^2 - 2.224e^{-06}z + 1.595e^{-09}}{-0.1156z^4 + 0.007188z^3 - 3.15e^{-06}z^2 + 2.053e^{-09}z - 9.28e^{-26}}$
$G_{vF}(s)$	$\frac{-7.352e^{-23}z + 5.293e^{-23}}{z^2 - 1.827z + 0.8283}$	$\frac{7.5z^9 - 12.39z^8 + 3.223z^7 + 1.662z^6 + 0.009921z^5}{z^9 - 1.519z^8 + 0.5082z^7 + 0.01183z^6 + 0.0009039z^5}$ $\frac{+0.003434z^4 - 1.711e^{-5}z^3 + 4.986e^{-8}z^2 - 1.44e^{-16}z + 1.217e^{-25}}{-6.997e^{-06}z^4 + 2.478e^{-8}z^3 - 6.58e^{-17}z^2 + 4.514e^{-26}z + 2.858e^{-43}}$

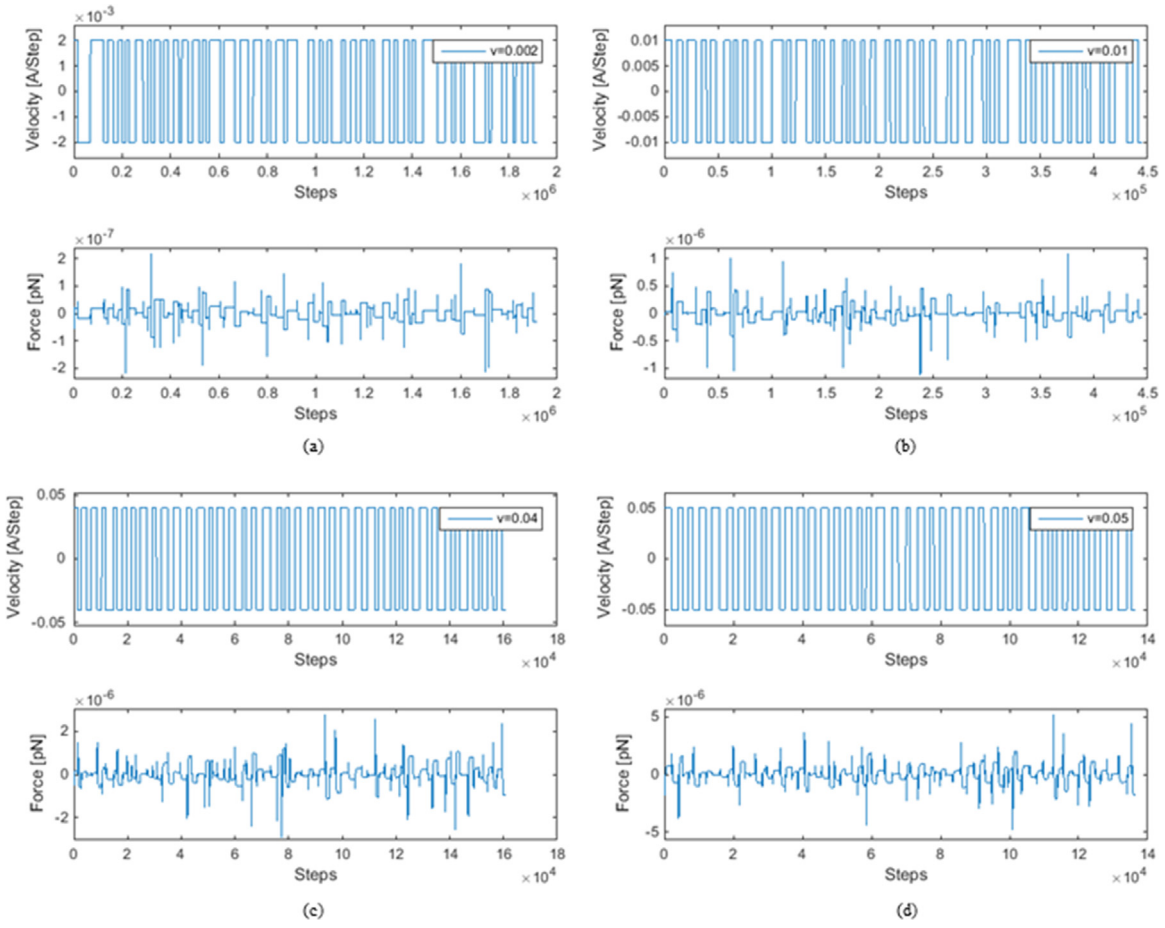

Fig. 10. Diagrams of velocity and interaction forces for different pulling velocities: (a) $v=0.002$[Å /Step], (b) $v=0.01$[Å /Step], (c) $v=0.04$[Å /Step], and (d) $v=0.05$[Å /Step].

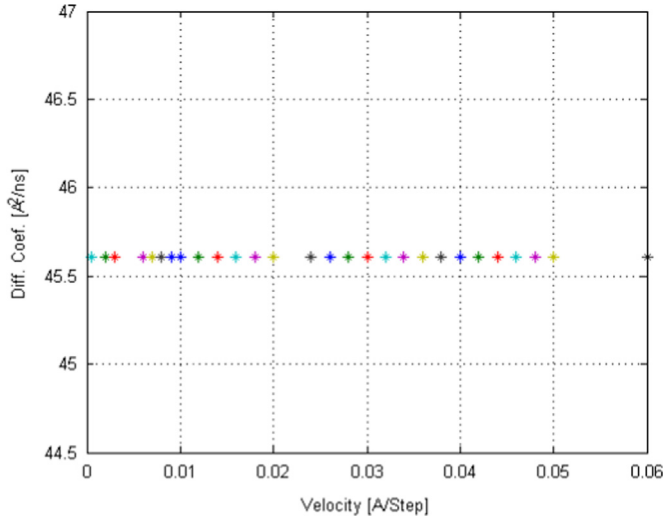

Fig. 11. Diffusion Coefficient of the membrane vs Pulling Velocity of the dummy atoms.

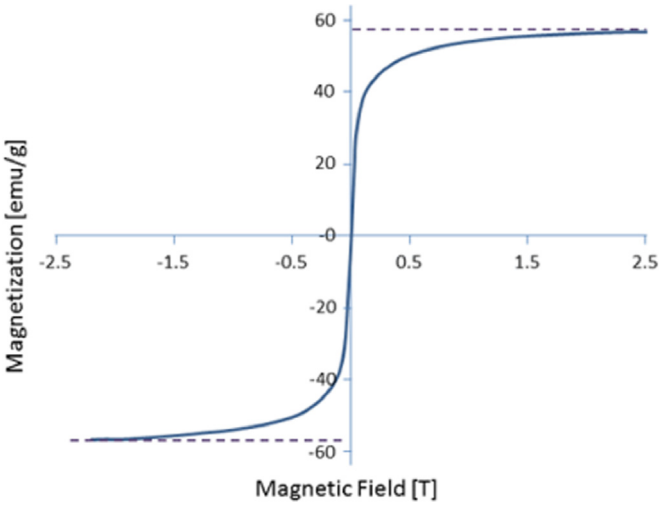

Fig. 12. Magnetization curve for Fe_3O_4/Au core/shell magnetic suspension.

already discussed, our results show that the calculated diffusion coefficient is independent of crossing velocity, thus it could be concluded that for other crossing durations that occur in different magnetic force fields and gradients, we will have a similar diffusion coefficient from the present method.

The magnetic force field strength of 1.5 [T] is a biologically relevant and non-invasive strength. Similar values in the range of 1.5–2 [T] have been frequently used in both computational models [14] and in-vivo studies [29] of MNP crossing through the BBB. Also the crossing time range of 1.5–7 min has a very good correlation with the near 5 minute time scale of experimental studies that have addressed MRI guided transcellular transport such as MNP-based Tumor cell labeling [30]. If we put aside the biochemical gateways to the brain that fall into an entirely different category of mechanisms in comparison with the external forced methods (such as the one studied in this research), there is only one major competitor for this method which is the ultrasound induced BBB opening. This method that can effectively breach the

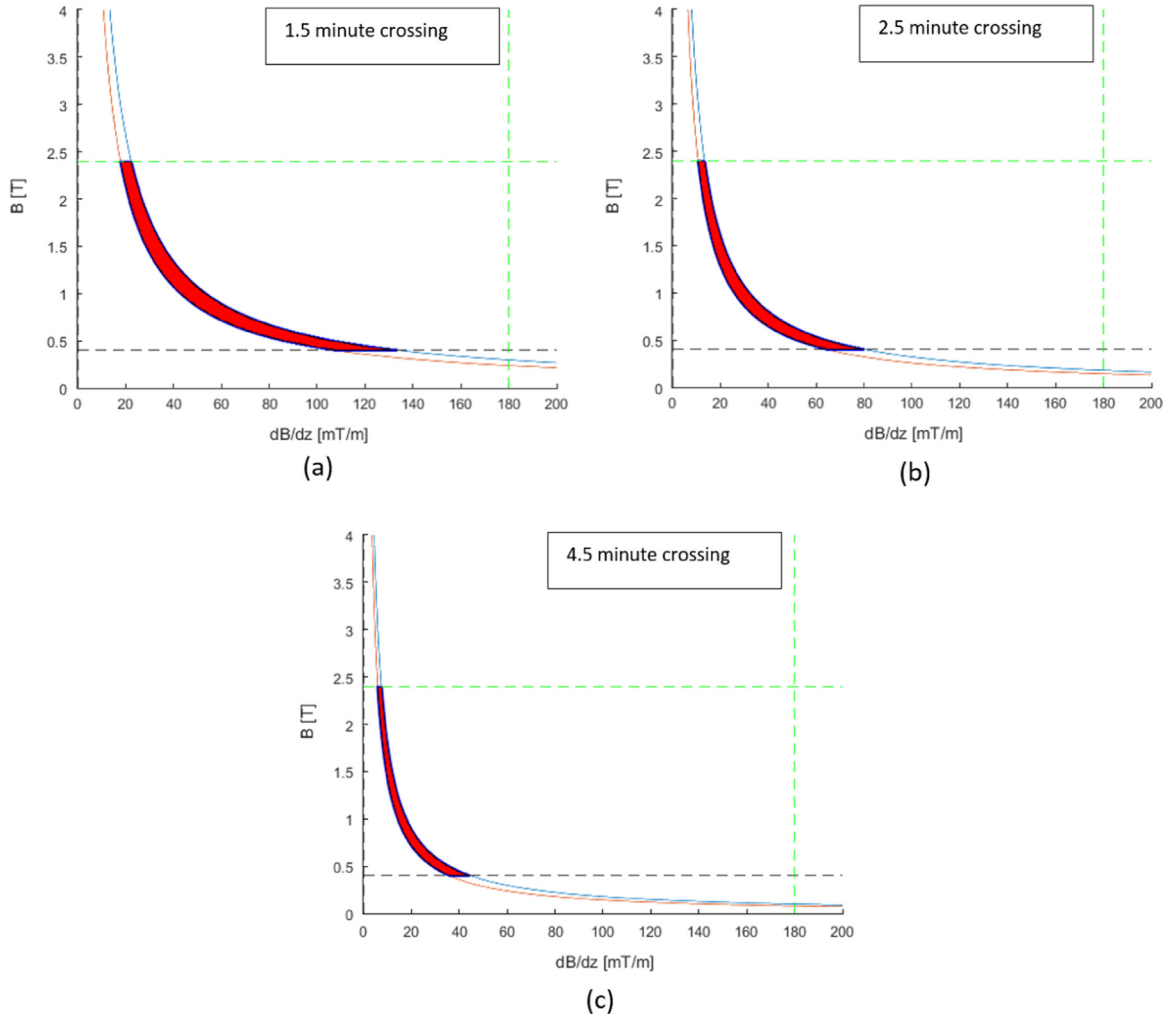

Fig. 13. Desirable area for the selection of magnetic field and magnetic gradients (a) for crossing in 1.5 min, (b) for crossing in 2.5 min and (c) for crossing in 4.5 min.

BBB, uses MRI guided focused ultrasound which also requires a similar 1.5 [T] magnetic force field [31]. However the ultimately high temperatures and pressures of the ultrasound microbubbles pose this method somewhat invasive for biological tissue.

7. Conclusions

In this work, we have studied the required interaction force profile which should be applied to the nano-particle in order for it to cross through the BBB. To achieve this target, we developed an atomic based model of the BBB. Two kinds of BBB membrane, POPC and DMPC have been studied. In addition, we have made a gold nano-particle in the sizes of 2 nm, 4 nm and 10 nm in diameter, besides, the nano-particle has been symmetrically coated with 18 segments of Thiol. The MD simulations have been carried out in order to extract the force required for crossing the NPs through the BBB. Therefore, the nano-particle has been supposed to move at a constant velocity through the BBB and the interaction force on the BBB membrane has been figured out. In experimental studies, the equivalent magnetic field can be substituted in order to shape the same force profile. The BBB membrane has been modeled in the frequency domain with a certain uncertainty around the linear model to cover all nonlinearity that was extracted in MD simulation. The simulation has been run for 1000 times in each velocity. The frequency domain for the BBB has been obtained, moreover, the diffusion coefficient has been extracted based on our model of the BBB system. In our future work, we will examine the effect of particle diameters in the force interaction and diffusion coefficient in order to find the best optimal magnetic field for crossing through the BBB.

Compliance with ethical standards

The authors declare that they have no conflict of interest.

References

[1] N. Joan Abbott, Adjanie A.K. Patabendige, Diana E.M. Dolman, Siti R. Yusof, David J. Begley, Structure and function of the blood–brain barrier, Neurobiol. Dis. 37 (1) (2010) 13–25.
[2] Toby W. Allen, Olaf S. Andersen, Benoit Roux, Ion permeation through a narrow channel: using gramicidin to ascertain all-atom molecular dynamics potential of mean force methodology and biomolecular force fields, Biophys. J. 90 (10) (2006) 3447–3468.
[3] Praveen Ballabh, Alex Braun, Maiken Nedergaard, The blood–brain barrier: an overview: structure, regulation, and clinical implications, Neurobiol. Dis. 16 (1) (2004) 1–13.
[4] Bastug Turgut, Serdar Kuyucak, Free energy simulations of single and double ion occupancy in gramicidin, J. Chem. Phys. 126 (10) (2007) 105103.
[5] Mattia Bramini, Dong Ye, Anna Hallerbach, Michelle Nic Raghnaill, Anna Salvati, Christoffer Åberg, Kenneth A. Dawson, Imaging approach to mechanistic study of nanoparticle interactions with the blood-brain barrier, ACS Nano (2014).
[6] Rune Brincker, Lingmi Zhang, Palle Andersen, Modal identification of output-only systems using frequency domain decomposition, Smart Mater. Struct. 10

(3) (2005) 441.
[7] James J. Choi, Jameel A. Feshitan, Babak Baseri, Shougang Wang, Yao-Sheng Tung, Mark A. Borden, Elisa E. Konofagou, Microbubble-size dependence of focused ultrasound-induced blood–brain barrier opening in mice in vivo, Biomed. Eng. IEEE Trans. 57 (1) (2010) 145–154.
[8] Cathrin J. Czupalla, Stefan Liebner, Kavi Devraj, Cerebral Angiogenesis: In Vitro Models of the Blood–brain Barrier, Springer 2014, pp. 415–437.
[9] G. De Fabritiis, P.V. Coveney, J. Villà-Freixa, Energetics of k+ permeability through gramicidin a by forward-reverse steered molecular dynamics, Proteins: Struct. Funct. Bioinforma. 73 (1) (2008) 185–194.
[10] Daan Frenkel, Berend Smit, Understanding Molecular Simulation: From Algorithms to Applications, Academic press, 2001.
[11] P. Garberg, Marguerite Ball, N. Borg, Roméo Cecchelli, Laurence Fenart, R. D. Hurst, T. Lindmark, A. Mabondzo, J.E. Nilsson, T.J. Raub, et al., In vitro models for the blood–brain barrier, Toxicol. Vitro 19 (3) (2005) 299–334.
[12] L.M. Griep, F. Wolbers, B. de Wagenaar, P.M. ter Braak, B.B. Weksler, Ignacio A. Romero, P.O. Couraud, I. Vermes, A.D. van der Meer, A. van den Berg, BBB on chip: microfluidic platform to mechanically and biochemically modulate blood-brain barrier function, Biomed. Microdevices 15 (1) (2013) 145–150.
[13] Daniela Guarnieri, Ornella Muscetti, Paolo A. Netti, A method for evaluating nanoparticle transport through the blood–brain barriain vitro, in: Drug Delivery System, Springer, 2014, pp. 185–199.
[14] Mustapha Hamdi and Antoine Ferreira. Computational study of superparamagnetic nanocapsules crossing the blood–brain barrier: a robotics approach, in: Proceedings of the IEEE/RSJ International Conference on Intelligent Robots and Systems (IROS), IEEE, 2012, pp. 2313–2318.
[15] Hummer Gerhard, Attila Szabo, Free energy reconstruction from nonequilibrium single-molecule pulling experiments, Proc. Natl. Acad. Sci. 98 (7) (2001) 3658–3661.
[16] Morten Ø. Jensen, Sanghyun Park, Emad Tajkhorshid, Klaus Schulten, Energetics of glycerol conduction through aquaglyceroporin Glpf, Proc. Natl. Acad. Sci. 99 (10) (2002) 6731–6736.
[17] Kyoungchul Kong, Masayoshi Tomizuka, Nominal model manipulation for enhancement of stability robustness for disturbance observer-based control systems, Int. J. Control., Autom. Syst. 11 (1) (2013) 12–20.
[18] Ioan Kosztin, Bogdan Barz, Lorant Janosi, Calculating potentials of mean force and diffusion coefficients from nonequilibrium processes without jarzynski's equality, J. Chem. Phys. 124 (6) (2006) 064106.
[19] P.R. Lockman, R.J. Mumper, M.A. Khan, D.D. Allen, Nanoparticle technology for drug delivery across the blood–brain barrier, Drug. Dev. Ind. Pharm. 28 (1) (2002) 1–13.
[20] Naik Pooja, Luca Cucullo, In vitro blood–brain barrier models: current and perspective technologies, J. Pharm. Sci. 101 (4) (2012) 1337–1354.
[21] Henrik Aalborg Nielsen, Henrik Madsen, Modelling the heat consumption in district heating systems using a grey-box approach, Energy Build. 38 (1) (2006) 63–71.
[22] Udo Seifert, Entropy production along a stochastic trajectory and an integral fluctuation theorem, Phys. Rev. Lett. 95 (4) (2005) 040602.
[23] Kaushik K. Shah, Li Yang, Thomas J. Abbruscato, In vitro models of the blood–brain barrier, in: Astrocytes, Springer, 2012, pp. 431–449.
[24] Jinglong Tang, Ling Xiong, Guofeng Zhou, Shuo Wang, Jianyu Wang, Li Liu, Jiage Li, Fuqiang Yuan, Songfang Lu, Ziyi Wan, et al., Silver nanoparticles crossing through and distribution in the blood–brain barrier in vitro, J. Nanosci. Nanotechnol. 10 (10) (2010) 6313–6317.
[25] Imola Wilhelm, Csilla Fazakas, Istvan A. Krizbai, In vitro models of the blood–brain barrier, Acta Neurobiol. Exp. 71 (1) (2011) 113–128.
[26] Kemin Zhou, John Comstock Doyle, Essentials of Robust Control, Prentice hall Upper Saddle River, NJ, 1998.
[27] Maysam Z. Pedram, Amir Shamloo, Ebrahim GhafarZadeh, Aria Alasty, Modeling and simulation of crossing magnetic nanoparticles through blood brain barrier (BBB), Conf. Proc. IEEE Eng. Med. Biol. Soc. 2014 (2014) 5280–5283.
[28] J.-B. Mathieu, S. Martel, Aggregation of magnetic microparticles in the context of targeted therapies actuated by a magnetic resonance imaging system, J. Appl. Phys. 106 (4) (2009).
[29] Weinberg, Irving N., et al., Non-invasive image-guided brain access with gradient propulsion of magnetic nanoparticles, in: Proceedings of the IEEE Nuclear Science Symposium and Medical Imaging Conference (NSS/MIC), 2012, IEEE, 2012.
[30] Brooks Hilary, Bernard Lebleu, Eric Vivès, Tat peptide-mediated cellular delivery: back to basics, Adv. Drug. Deliv. Rev. 57 (4) (2005) 559–577.
[31] Nathan McDannold, et al., MRI-guided targeted blood-brain barrier disruption with focused ultrasound: histological findings in rabbits, Ultrasound Med. Biol. 31 (11) (2005) 1527–1537.